Asian Journal of Chemistry; Vol. 27, No. 4 (2015), 1513-1520

ASIAN JOURNAL OF CHEMISTRY

http://dx.doi.org/10.14233/ajchem.2015.18607

Preparation of Activated Carbon from Pyrolytic Residue of Rice Husk and Its Application for the Adsorption of Phenol and Iodine

XIAN ZHANG, HUIHUI LIU, YAXIN LI, GUIYING LI* and CHANGWEI HU*

Key Laboratory of Green Chemistry and Technology, Ministry of Education, College of Chemistry, Sichuan University, Chengdu 610064, P.R. China

*Corresponding authors: Tel/Fax: +86 28 85411105; E-mail: changweihu@scu.edu.cn

Received: 16 August 2014; *Accepted*: 11 November 2014; *Published online*: 4 February 2015; AJC-16826

The solid residue from the pyrolytic liquefaction of rice husk, known as pyrolytic carbon, was used as starting material to prepare activated carbon. Pyrolytic carbon was pretreated by NaOH solution at 100 °C for 5 h to remove SiO_2, thereby obtaining samples with low surface area. The samples were activated under N_2 atmosphere at 650, 700, 750, 800, or 850 °C with different activation times, obtaining activated carbon samples. Activated carbon samples were characterized by BET, XRD and SEM. The optimized conditions were the following: 750 °C activation under N_2 for 1.5 h. The prepared activated carbon had a surface area of 470 m^2 g^{-1}. The highest phenol adsorption capacity of the activated carbon from water was 60.98 mg g^{-1} and the iodine adsorption capacity reached 586.30 mg g^{-1}. The pseudo-second order kinetics and Langmuir models were determined to fit the adsorption experimental data.

Keywords: Pyrolytic carbon, Activated carbon, BET, Phenol adsorption, Iodine adsorption.

INTRODUCTION

Rice husk (RH) is an agricultural residue abundantly available in rice-producing countries. The annual worldwide output has been estimated to be 80 million tons, of which approximately half is generated in China[1]. However, there is only a little research concerning its utilization. If this agricultural residue is not utilized properly, tremendous waste will be produced, causing energy loss and environmental pollution. At the same time, because of the distinct advantages of large specific surface areas and hydrophobic nature, large pore volume and broad pore size distribution, carbonaceous materials, *e.g.*, activated carbon, have been widely employed as adsorbents to remove pollutants[2,3]. An economic approach is the utilization of agricultural waste biomass (*e.g.*, rice husk, corncob, straw and cotton stalks) as precursors for the preparation of activated carbon. Slow pyrolysis of biomass at high temperature is widely used to produce low-cost activated carbon[4]. Physical and chemical activation are the two fundamentally employed methods for the preparation of activated carbons. Physical activation involves reaction at high temperatures in steam or carbon dioxide[5,6]. In chemical activation, raw material is mixed with an activator, presenting several advantages, including lower reaction temperature and better pore structure[7]. The dried rice husk was carbonized at 350 to 500 °C in a nitrogen atmosphere and the carbonized product was heated in the presence of a substantial weight of potassium hydroxide or sodium hydroxide at 350 to 400 °C for 0.3 to 1.0 h to dehydrate the combination. The temperature was then raised to 650 to 850 °C for 1 h to activate the combination. The obtained activated carbon had extremely high surface area (1413-3014 m^2 g^{-1})[8]. However, hydrogen and silicon elements in the material were not used. There are several disadvantages of the chemical activation process, such as the corrosiveness of the process, the huge amount of water needed in the washing steps and the high cost, especially with strong base as the activator, which exhibits serious corrosion activity toward the reactor.

The production of activated carbon from rice husk cannot make full use of the raw materials. Rice husk has been used to produce bio oil *via* pyrolysis[9], with the production of a large amount of rice husk residual powder (PC) as the by-product. The study to make pyrolytic carbon value added has great significance. The main components of the pyrolytic carbon are carbon and silicon. Synthesis of high specific surface area silica from pyrolytic carbon by precipitation at low pH has been researched[10], but carbon has not been fully used. If pyrolytic carbon can be used to produce activated carbon, it can not only solve the problem of pollution but also take full advantage of raw material, *i.e.*, the components of rice husk are totally used, producing both energy material (bio-oil) and useful activated carbon. At the same time, the activated carbon produced could be used in the removal of pollutants from aqueous solution as an ideal adsorbent.

In this study, activated carbon samples were prepared using pyrolytic carbon in an attempt to make full use of the rice husk. The performance for the adsorption of phenol and iodine in water by the prepared activated carbon was also discussed.

EXPERIMENTAL

Raw materials and preparation of activated carbon: Pyrolytic carbon (PC) was produced from rice husk in a fluidized bed reactor, where the rice husk was exposed to 475 °C for less than 2 s[9]. Sodium hydroxide, phenol and iodine were of analytical grade purchased from Ke Long chemical reagent factory of Chengdu and were used without further purification.

The pyrolytic carbon with a particle size of 40 to 80 mesh was washed by distilled water and dried at 110 °C for 24 h. The preparation of activated carbon samples proceeded *via* two steps. Firstly, 20 g pyrolytic carbon was mixed with 200 mL of aqueous solution of NaOH of different concentrations (4, 5 and 6 mol L^{-1}) and the mixture was kept at 100 °C for 5 h. Next, the mixture was filtered using filter paper and the filtrate of the sodium silicate solution could be used to produce silica[10]. The residue was washed with water to reach a constant pH of approximately 7 and dried at 110 °C for 24 h. Secondly, the solid samples obtained from the first step were introduced into a tube reactor and heated from room temperature to the final activation temperature under nitrogen flow of 30 mL min^{-1}. The samples were kept at the final temperature for various activation times before cooling to room temperature. The activation temperatures used were 650, 700, 750, 800 and 850 °C. The activation times selected were 0.5, 1, 1.5, 2 and 2.5 h. The resultant samples were denoted as Cx-y (where x is the concentration of the NaOH solution, mol L^{-1} and y is the activation temperature, °C).

Elemental analysis: Elemental analysis was performed to accurately characterize the pyrolytic carbon using FLASH 1112 SERIES. The major elements C, H and N of the sample were determined.

ICP-AES analysis: An IRIS Advantage ICP-AES was used to analyze the amount of metal elements contained in the pyrolytic carbon. A 0.20 g sample was burnt to ash at 800 °C for 3 h in air atmosphere. The obtained ash was dissolved in a 1:1 hydrochloric acid solution and further diluted to 100 mL with distilled water. Thus, the metal contents could be obtained by analyzing their concentrations in the solution[11].

Nitrogen adsorption/desorption: The specific surface area and pore size distributions of the activated carbon samples were measured by N_2 adsorption at -196 °C using a Micromeritics TriStar 3020 instrument. Adsorption data were obtained over a range relative pressure, P/P_0, ranging from approximately 10^{-5} to 1. The micropore volume (Vmic), micropore surface area (Smic) and external surface area (Sext) were calculated using the t-plot method. The average pore diameter was estimated from the surface area and pore volume[11,12]. Prior to the gas adsorption measurements, the samples were degassed at 120 °C for 1.5 h and 300 °C for 2.5 h in vacuum condition until a pressure of less than 10^{-2} Pa.

X-ray powder diffraction: The XRD measurement was operated on a DANDONG FANGYUAN DX-1000 instrument with CuK_α radiation operated at 40 kV and 25 mA. The diffracted intensity was measured over the 2θ range from 5° to 80°.

Scanning electron microscopy: Scanning electron microscopy was used to observe the morphological features of the activated carbon samples. The experiment was performed on an INSPECTF with an acceleration voltage of 20 kV.

Phenol adsorption experiment: For the adsorption experiment, 0.10 g activated carbon was placed in a conical flask and 0.10 L aqueous solution of phenol (42 mg L^{-1}) was added. The adsorption of phenol from the aqueous solutions was performed in a 250 mL conical flask placed in a water bath at 35 °C. The adsorption solutions with activated carbon were stirred with uniform stirring speed (4 r s^{-1}) in all the experiments. The concentration of phenol was analyzed every 15 min within the first 2 h. After 2 h, the concentration analysis was performed every 0.5 h until reaching equilibrium. The concentration of the remained phenol in the aqueous phase was quantified using a HITACHI U-4100 UV-visible spectrophotometer at a wavelength of 270 nm[13]. The adsorption capacity q_e (mg g^{-1}) of phenol was calculated using the following equation:

$$q_e = \frac{(C_0 - C_e)V}{M} \quad (1)$$

where C_0 and C_e are the initial and equilibrium phenol concentrations (mg L^{-1}), V is the volume of phenol solution (L) and M is the mass of the activated carbon sample (g).

Phenol adsorption experiment: To investigate the adsorption isotherms of phenol, a batch of phenol solutions with different concentrations (20, 40, 60, 80 and 100 mg L^{-1}) were prepared and 0.10 g C4-750 was put into 100 mL of the prepared phenol solutions. The mixture in the 250 mL conical flasks was stirred at 4 r s^{-1} throughout all the experiments. The phenol concentration remaining in aqueous solution was analyzed quantitatively using a HITACHI U-4100 UV-visible spectrophotometer at a wavelength of 270 nm until reaching equilibrium. The adsorption isotherms of phenols on the activated carbon samples were studied at 298, 308, 318, 328 and 338 K.

I_2 Adsorption experiment: The I_2 adsorption experiments were conducted according to the Chinese National Standards GB/T 12496.8-1999. Firstly, the activated carbon sample was dried at 110 °C for 24 h and 0.50 g of dried activated carbon sample and 50 mL I_2 solution were added to a 250 mL flask, which was placed in a thermostat at room temperature (25 ± 1 °C). The solution with activated carbon was stirred for 15 min. Next, the mixture was filtered using filter paper to obtain the I_2 adsorption capacity by titrating the residual I_2 concentration of the filtrate.

RESULTS AND DISCUSSION

Characterization of the raw material pyrolytic carbon: The results of the elemental analysis showed that the raw material pyrolytic carbon contained 44.5 % carbon, 2.3 % hydrogen and 0.5 % nitrogen. In addition, minor other mineral compositions were also included in the pyrolytic carbon. As shown in Table-1, the contents of aluminum, calcium, iron, potassium, sodium and magnesium were 0.03, 0.69, 0.14, 0.27, 0.11 and 0.11 %, respectively. Beside the above components,

TABLE-1
METAL CONTENT OF PYROLYTIC CARBON DETERMINED BY ICP

Sample	Al (%)	Ca (%)	Fe (%)	K (%)	Na (%)	Mg (%)
Pyrolytic carbon	0.03	0.69	0.14	0.27	0.11	0.11

the rest of the main component was silica (about 51.35 %). The carbon content of commercial activated carbon was usually more than 70 %[14], thus the silica contained in pyrolytic carbon needed to be removed for activated carbon production. Treatment with NaOH solution was usually used to remove silica[15,16] and this method was adopted in the present work.

Effects of the activation conditions on the properties of activated carbon

Effects of the activation temperature and concentration of the NaOH solution: A series of activated carbon samples were prepared by activation at different temperatures. Fig. 1(a) and (b) present the adsorption-desorption isotherms of N_2 and the pore size distributions for the samples. The N_2 adsorption isotherms shown in Fig. 1(a) correspond to typical type I in the BDDT classification[17], which indicated that all the samples were micropore materials. The hysteresis loops in the nitrogen isotherm represented the existence of mesoporosity and the hysteresis loops of the parallel adsorption and desorption branches were indicative of slit-shaped pores[14,18]. The activated carbon samples were similar to commercially available coal-based activated carbon from Jiangsu Nantong Activated Carbon Cooperation (China)[11]. The pore size distributions were largely dependent on the activation temperature. The average pore diameters of the activated carbon samples between 19.0 and 20.8 Å principally denoted micropores. Table-2 shows the BET surface areas of the pyrolytic carbon and activated carbon samples obtained by treatment with different concentrations of NaOH solution and heated under N_2 atmosphere at different temperatures. As seen in Table-2, pyrolytic carbon had a low specific surface area (31 $m^2 g^{-1}$) and micropore volume (0.008 $cm^3 g^{-1}$). With the increase of the activation temperature, the surface area of the activated carbon samples increased, reached the maximum at 750 °C and then decreased. The highest specific surface area could reach 470 $m^2 g^{-1}$. Compared with the raw materials that had only 31 $m^2 g^{-1}$, the specific surface area increased greatly. The micropore surface areas also increased from 18 to 405 $m^2 g^{-1}$.

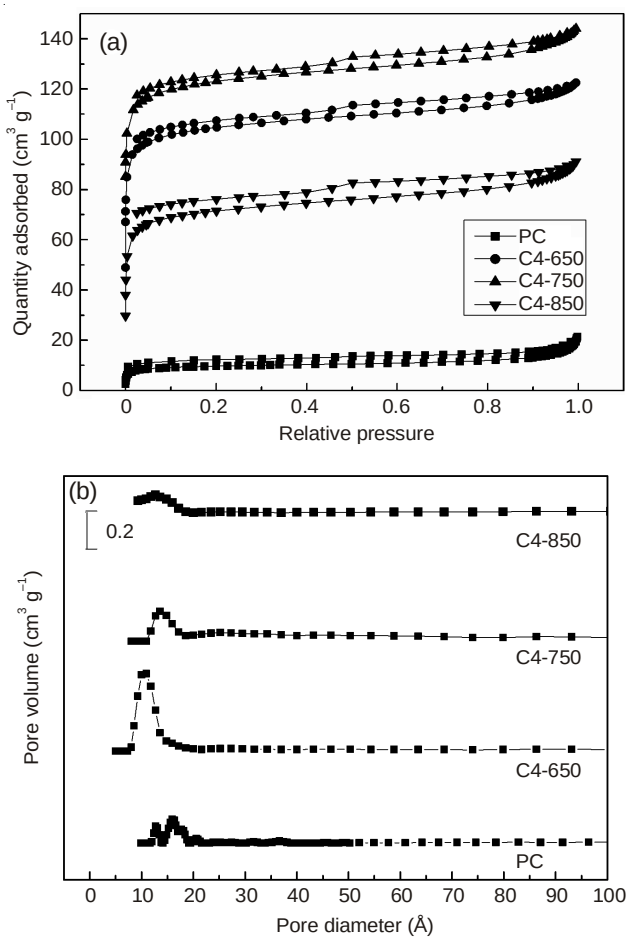

Fig. 1. Adsorption-desorption isotherms of N_2 (a) and pore size distributions for pyrolytic carbon and activated carbon samples (b)

TABLE-2
TEXTURAL CHARACTERISTICS OF THE DIFFERENT SAMPLES[a]

Sample	A_{BET} ($m^2 g^{-1}$)	A_{mic} ($m^2 g^{-1}$)	A_{ext} ($m^2 g^{-1}$)	V_{mic} ($cm^3 g^{-1}$)	Average pore width (Å)
PC	31	18	13	0.008	17.6
C4-650	366	322	44	0.130	19.3
C4-700	424	369	55	0.149	19.1
C4-750	470	405	65	0.168	19.2
C4-800	443	389	34	0.163	18.6
C4-850	278	225	43	0.092	19.8
C5-650	398	351	47	0.142	19.1
C5-700	461	403	58	0.163	19.0
C5-750	467	415	52	0.168	19.1
C5-800	381	336	45	0.135	19.4
C5-850	271	228	43	0.092	20.8
C6-650	319	283	36	0.114	19.0
C6-700	407	362	45	0.146	18.9
C6-750	460	406	54	0.164	19.2
C6-800	271	228	43	0.092	19.4
C6-850	224	170	54	0.069	23.5

[a]Activated time was 1.5 h; PY = Pyrolytic carbon

The micropore volumes of the activated carbon samples increased from 0.008 to 0.168 $cm^3 g^{-1}$. The same temperature regulation appeared in all the activated carbon samples obtained by treatment with different concentrations of NaOH solution. The specific surface area of C5-750 and C6-750 were 467 and 460 $m^2 g^{-1}$, respectively. They were higher than those for the samples treated with the same concentration of NaOH solution and activated at other temperatures.

The goal of using high concentration NaOH solution was to dissolve silica better[15] and a high concentration of sodium silicate solution was helpful for further processing. The effect of the NaOH concentration on this reaction was not obvious within the concentration range used. The samples treated with different concentrations of NaOH solution had similar BET values if the activation temperature was the same. Considering drug consumption, the NaOH concentration of 4 mol L^{-1} and calcination temperature of 750 °C were chosen as optimal conditions.

Activation time: A series of activated carbon samples were produced with different activation times. The effect of activation time on the surface area was illustrated in Table-3. It was shown that activation time significantly affected the surface area. With the increase of activation time, the surface area of the activated carbon samples increased firstly and then reached the maximum value at 2 h. Prolonged activation time led to decrease of surface area. The specific surface areas of the samples obtained with 1.5 and 2 h were similar, *i.e.*, 470 and 478 $m^2 g^{-1}$, only a 8 $m^2 g^{-1}$ difference. At the same time, the *t*-Plot micropore volume of the 1.5 h sample was larger than the 2 h sample, which was 0.168 $cm^3 g^{-1}$. These differently activated samples had similar average pore widths, ranging from 19.0 to 19.4 Å. A time of 1.5 h was chosen as the optimal activation time, considering energy consumption.

XRD analysis: The X-ray diffraction patterns of the carbon samples were obtained and are shown in Fig. 2. Two insignificant peaks at approximately 2θ = 26.2° and 44.3° were assigned to the diffraction of the (002) (d002 = 0.339 nm) and (100) planes (d100 = 0.204 nm) in carbon, respectively. This indicated the formation of a structure of amorphous carbon[16]. Comparison of the XRD peaks of pyrolytic carbon and C4-750, showed that a shoulder peak of a broad peak at 2θ = 26.2° centered at the 2θ angle of 22° was observed in pyrolytic carbon sample and it indicated the presence of completely amorphous silica[19]. This result showed that, after NaOH treatment, silica in the C4-750 had been basically removed. The intensity of the peak at 2θ = 44° on C4-750 became stronger, indicating that the pores are also created by the decomposition of carbon structures along the direction of the graphitic structures[19].

SEM analysis: Fig. 3a shows the morphological features of the raw material pyrolytic carbon. Pyrolytic carbon showed

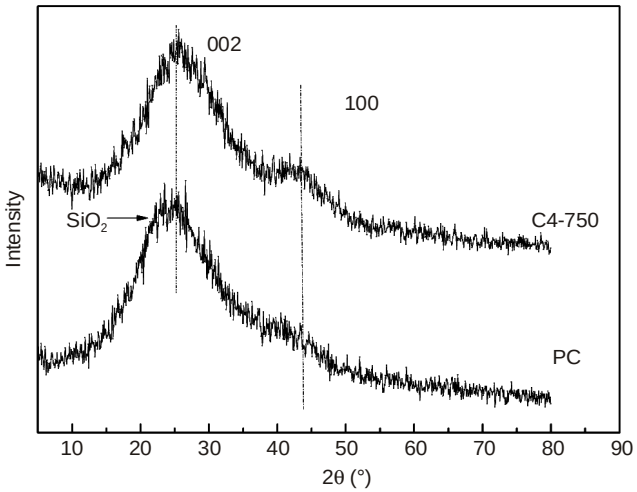

Fig. 2. XRD of pyrolytic carbon and C4-750

organized fragment morphology, such as rolling hills, in which the outer epidermis of the rice husk was covered with an organized corrugated structure. It was the so-called "vascular bundle structure"[16,20] that contained cellulose, lignin and SiO_2. Comparing Fig. 3a2 (pyrolytic carbon) with Fig. 3b2 (C4-750), the C4-750 was much rougher than pyrolytic carbon. C4-750 after NaOH solution treatment and activation at 750 °C in N_2 had lost SiO_2 and formed many pores inside. High temperature damaged the structure of pyrolytic carbon and created many cracks and pores on the activated carbon sample. A comparison of Fig. 3a3 with Fig. 3b3 showed that C4-750 had more pores, which was consistent with the results of the specific surface area. When the carbon sample was subjected to the activation temperature of 750 °C, most of the volatiles in the sample were removed, leading to the production of small pores and achieving a high specific surface area.

Adsorption of phenol from aqueous solution

Kinetics of phenol adsorption: The sorption capacity was one of the most important parameter of the adsorption characteristics and the adsorption kinetics was the second feature that might also strongly constrain the applicability of the adsorption. The low adsorption kinetics significantly lengthened the operation time, which made the removal processes unfavorable[21]. The adsorption of phenol on the activated carbon samples as a function of time is shown in Fig. 4. The process was rapid in the initial period and then became slow with increasing contact time. The equilibrium sorption capacity was obtained at 2 h. The adsorption quantity of the samples was directly related to their specific surface area. As the specific surface area increased, the adsorption quantity of the sample increased. The C4-750 had the largest phenol adsorption quantity of 18 mg g^{-1}. The adsorption processes of C4-700

TABLE-3
EFFECT OF THE ACTIVATED TIME ON THE TEXTURAL CHARACTERISTICS OF THE C4-750 SAMPLE

Activated time (h)	A_{BET} ($m^2 g^{-1}$)	A_{mic} ($m^2 g^{-1}$)	A_{ext} ($m^2 g^{-1}$)	V_{mic} ($cm^3 g^{-1}$)	Average pore width (Å)
0.5	358	321	37	0.129	19.2
1.0	446	356	50	0.159	19.1
1.5	470	405	65	0.168	19.2
2.0	478	411	67	0.166	19.4
2.5	426	377	49	0.152	19.0

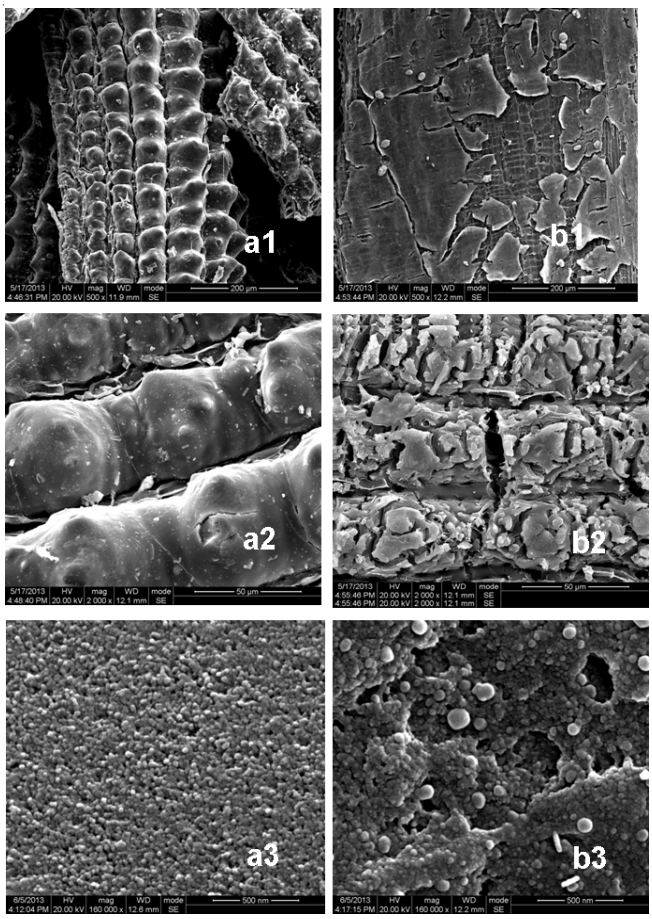

Fig. 3. SEM images of pyrolytic carbon (a1-a3) and C4-750 (b1-b3) samples

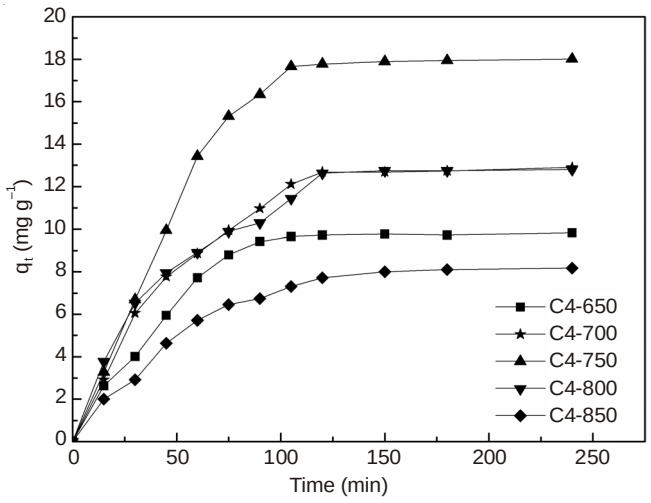

Fig. 4. Adsorption kinetics of phenols on activated carbon samples: 35 °C, initial concentration 42 mg L^{-1}

and C4-800 were similar and their equilibrium adsorption quantities were 12.9 and 12.8 mg g^{-1}. C4-650 had the equilibrium adsorption quantity of 9.8 mg g^{-1} and adsorption quantity of C4-850 was only 8.2 mg g^{-1}. Because phenol (size of phenol = 0.8 nm) was adsorbed mainly within the micropores, the high adsorption capacity of activated carbon was attributed to its high micropore volume percentage[22]. The micropore volume of C4-750 was 0.168 cm^3 g^{-1}, which was the highest among the activated carbon samples; thus, the adsorption of phenol on C4-750 was also the biggest.

The pseudo-first order (Lagergren) and pseudo-second order models are the most commonly used kinetic models to describe phenol adsorption[23,24]. The Lagergren model is expressed by eqn. 2, whereas the pseudo-second order model is given by eqn. 3:

$$\ln (q_{e\,exp}-q_t) = \ln q_e - K_1 t \quad (2)$$

$$\frac{t}{q_t} = \frac{1}{k_2 q_e^{\,2}} + \frac{t}{q_e} \quad (3)$$

where t and q_t are the time (min) and the amount of phenol adsorbed by carbon at time t (mg g^{-1}), $q_{e\,exp}$ is the amount of phenol adsorbed experimentally at equilibrium and q_e is the calculated equilibrium; both are expressed as mg g^{-1}. k_1 is the rate constant of the pseudo-first order kinetic model (min^{-1}) and k_2 is the rate constant of the pseudo-second order kinetic model (g min^{-1} mg^{-1}).

A comparison of the data obtained by the two models is given in Table-4. The correlation coefficients (R^2) for the Lagergren equation were low. Furthermore, the experimental $q_{e\,exp}$ values did not agree well with the calculated ones, whereas the linear plot of the pseudo-second order model showed a very good fit with the experimental data with R^2 all above 0.975, indicating that the pseudo-second order model was more suitable for the adsorption of phenol and the calculated q_e was close to the experimental value. This indicated that the rate determining step was not the external diffusion of phenol from the bulk liquid to the carbon surface but might involve one or more of the internal steps[23,25].

Adsorption isotherms of phenol: An adsorption isotherm shows the distribution of adsorbed molecules between solid and liquid phases at equilibrium[26]. The results of the adsorption isotherms are presented in Table-5. Three widely used models, Langmuir, Freundlich and D-R isotherm, were applied to the fitting of the experimental data. The Langmuir model is based on the assumption of a homogeneous adsorbent surface with identical adsorption sites, which could be written as:

$$q_e = \frac{K_L q_m C_e}{1 + K_L C_e} \quad (4)$$

TABLE-4
COMPARISON OF THE PSEUDO-FIRST AND PSEUDO-SECOND ORDER KINETIC MODELS OF PHENOL ADSORPTION

Samples	$q_{e\,exp}$ (mg g^{-1})	Pseudo-first-order			Pseudo-secend-order		
		q_e(cal) (mg g^{-1})	k_1 (min^{-1})	R^2	q_e(cal) (mg g^{-1})	$10^3 \times k_2$ (g $mg^{-1}min^{-1}$)	R^2
C4-650	9.8	10.46	0.033	0.852	9.87	7.1	0.983
C4-700	12.9	15.14	0.027	0.936	15.38	1.9	0.984
C4-750	18.0	29.37	0.037	0.881	20.96	1.6	0.976
C4-800	12.8	17.38	0.030	0.786	15.55	1.6	0.990
C4-850	8.2	9.38	0.060	0.829	8.29	2.0	0.986

TABLE-5
LANGMUIR, FREUNDLICH AND D–R PARAMETERS FOR PHENOL ADSORPTION ON ACTIVATED CARBON

Sample	Temperature (K)	Langmuir adsorption isotherm			Freundlich adsorption isotherm			D-R isotherm		
		q_m (mg g^{-1})	$10^2 \times K_L$ (L mg^{-1})	R^2	n	K_F (mg g^{-1}) (L $mg^{-1})^{1/n}$	R^2	q_m (mg g^{-1})	E (kJ mol^{-1})	R^2
C4-750	298	28.09	3.06	0.989	2.06	1.90	0.945	19.24	0.726	0.970
	308	43.29	2.26	0.999	2.69	3.25	0.978	21.77	0.642	0.901
	318	45.46	2.25	0.993	1.75	3.29	0.974	26.65	1.258	0.930
	328	57.47	1.31	0.997	1.66	1.61	0.969	32.83	0.533	0.920
	338	60.98	2.50	0.997	1.65	3.83	0.976	34.47	0.631	0.910

where q_m is the maximal adsorption capacity, K_L is a constant related to the free energy of the adsorption. The Langmuir model is used for homogenous surfaces and demonstrates monolayer coverage of the adsorbate at the outer surface of the adsorbent[21].

Freundlich model is an empirical equation assuming heterogeneous adsorptive energies on the adsorbent surface, which could be written as:

$$q_e = K_F C_e^{\frac{1}{n}} \quad (5)$$

where K_F and n are the Freundlich constants related to the adsorption capacity and adsorption intensity, respectively. The Freundlich isotherm indicates that significant adsorption occurred at low concentrations, but the increase in the amount adsorbed with concentration became less significant at higher concentration[22]. The D-R isotherm can be described as follows[27]:

$$\ln q_e = \ln q_m - \beta\varepsilon^2 \quad (6)$$

$$E = \frac{1}{\sqrt{2\beta}} \quad (7)$$

where β is a constant related to the mean free energy of adsorption per mole of the adsorbate ($mol^2\ kJ^{-2}$) and E is the mean free energy of adsorption per mole of the adsorbate (kJ mol^{-1}). q_m is the saturation capacity in theory and ε is the polanyi potential, which is equal to RT ln (1 + 1/C_e), where R (J mol^{-1} K^{-1}) and T (K) are the gas constant and the absolute temperature, respectively.

A linearized plot of C_e *versus* q_e is widely used to correlate the derivation of various isotherms and provide reasonable interpretation of the experimental data[24]. As shown in Fig. 5, the residual equilibrium concentration of phenol in solution was increased with increasing initial solution concentration. At the same time, the equilibrium isotherm constants and correlation coefficients obtained from the linear fits of the Langmuir, Freundlich and D-R isotherms are given in Table-5. The linear relationship of the experimental data was calculated using the three different equations. As shown in Table-5, the Langmuir isotherm best described the experimental data, which was apparent from the values of the correlation coefficient (R^2) under 298, 308, 318, 328 and 338 K, implying the surface homogeneity of the adsorbent. The experimental data matched the Langmuir model better than the Freundlich and D-R models. The Langmuir equation was reasonably applicable in all of the cases with correlation coefficients (R^2) in the range of 0.989-0.999, which were higher than those of the Freundlich model and D-R model. With the rise of temperature, the q_m value showed increases for phenol of 28.09, 43.29, 45.46, 57.47 and 60.98 mg L^{-1}, which indicated that the prepared activated carbon possessed relatively homogeneous surface for the adsorption of phenol.

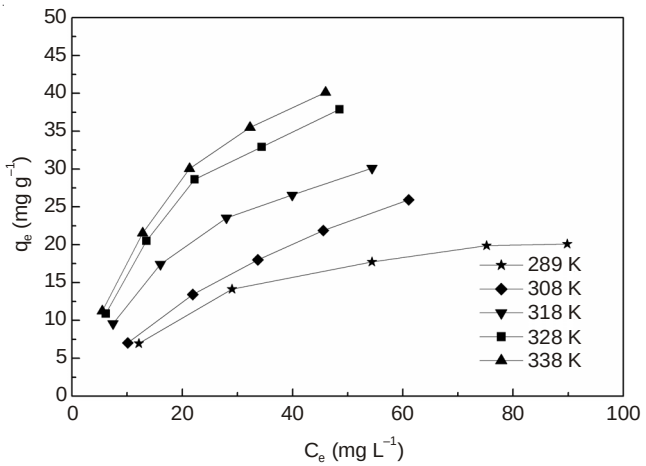

Fig. 5. Adsorption isotherms of phenol on C4-750 at different temperature

Adsorption thermodynamics: Adsorption experiments at different temperatures were also performed to evaluate the influence of temperature (298-338 K). The thermodynamic properties of the adsorbent (C4-750) system were calculated using the following equations[28]:

$$K_d = \frac{q_e}{C_e} \times 1000 \quad (8)$$

$$\ln K_0 = \frac{\Delta S^0}{R} - \frac{\Delta H^0}{RT} \quad (9)$$

where ΔS^0 and ΔH^0 are the values of the entropy change and the enthalpy change in the process, R (8.314 J $mol^{-1}K^{-1}$) is the universal gas constant, T (K) is the absolute temperature and K_d is the distribution coefficient. The thermodynamic parameters could be evaluated from the variation of the thermodynamic equilibrium constant K_0 with the change in temperature 29 and K_0 is computed from the intercept of the plot of ln K_d *versus* C_e. The free energy change (ΔG^0) is defined as follows for the adsorption reactions:

$$\Delta G^0 = -RT \ln K_0 \quad (10)$$

Furthermore, the value of the free energy change ΔG^0 could be calculated[29]. The values of ΔS^0, ΔH^0 and ΔG^0 were computed from the slope and intercept of the plot of ln K_0 *versus* 1/T, as shown in Fig. 6. The calculated values of ΔS^0, ΔH^0 and ΔG^0 are shown in Table-6. The values of ΔG^0 were -16.138, -16.977, -19.246, -20.715, -21.673 kJ/mol at five

different temperatures. The negative values of ΔG^0 showed the spontaneous nature of the process with phenol adsorbed onto the C4-750 sample[29]. The value of ΔS^0 was 148.38 J $mol^{-1}K^{-1}$. The positive value of ΔS^0 indicated the spontaneity of the C4-750 sample for phenol and an increasing randomness at the solid-solution interface in the adsorption reaction[30]. The positive value of ΔH^0 (28.235 kJ mol^{-1}) implied that the adsorption process was an endothermic reaction[30,31], which was supported by the increasing adsorption of phenol with the increase of the temperature.

TABLE-6
THERMODYNAMIC PARAMETERS FOR C4-750 ADSORPTION OF PHENOL

T (K)	ln K_0	ΔG^0 (kJ mol^{-1})	ΔH^0 (kJ mol^{-1})	ΔS^0 (J $mol^{-1}K^{-1}$)
298	6.51	-16.138		
308	6.63	-16.977		
318	7.28	-19.246	28.235	148.38
328	7.60	-20.715		
338	7.71	-21.673		

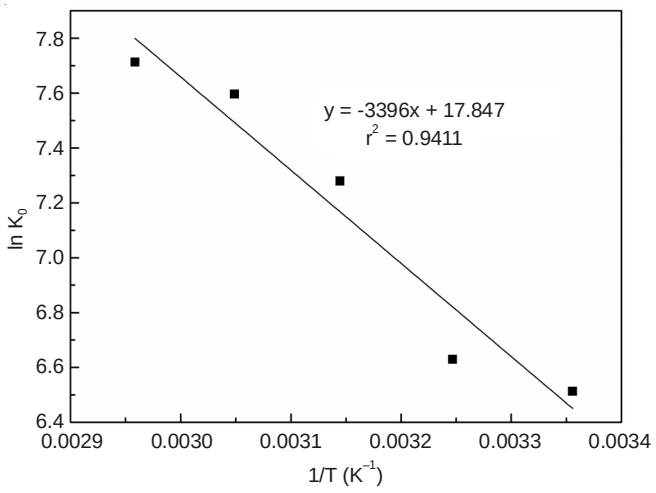

Fig. 6. Plot of ln K_0 *versus* 1/T on C4-750 adsorb phenol

Adsorption of I_2: Table-7 shows the iodine adsorption capacity of the activated carbon samples activated with different temperatures. The adsorption capacity q (mg g^{-1}) of I_2 was calculated using the following equation:

$$q = \frac{(C_0 - C)VM}{m} \quad (11)$$

where C_0 and C are the initial and final I_2 concentrations (mol L^{-1}), V is the volume of the I_2 solution (L), M is the molar mass of I_2 (mol g^{-1}) and m is the mass of the activated carbon sample (g). The C4-650 sample had the minimum iodine adsorption capacity (395.94 mg g^{-1}). With the increment of the activation temperature, the iodine adsorption capacity gradually increased and the iodine adsorption capacity reached its maximum of 586.30 mg g^{-1} at an activation temperature of 750 °C. The increase in the iodine adsorption capacity was most likely related to the increase of the surface area. The iodine adsorption capacities of C4-800 and C4-850 were 583.76 and 545.69 mg g^{-1}, respectively. Therefore, the iodine adsorption capacity decreased with the increment of the activation temperature.

TABLE-7
IODINE ADSORPTION VALUES OF THE DIFFERENT SAMPLES

Samples	Iodine adsorption value (mg g^{-1})
C4-650	395.94
C4-700	489.85
C4-750	586.30
C4-800	583.76
C4-850	545.69

Conclusion

For the preparation of activated carbon from pyrolytic carbon, the optimal activation temperature was 750 °C and the optimal activation time was 1.5 h. The prepared activated carbon had a surface area of 470 m^2 g^{-1} and an average pore size of 19.2 Å. This method is simple and has low cost with little corrosion of the equipment. The adsorption of phenol on the activated carbon samples adhered to a pseudo-second order kinetics model and the Langmuir adsorption isotherm. The correlation coefficients (R^2) were all above 0.975. The q_m values at different temperatures were 28.09, 43.29, 45.46, 57.47 and 60.98 mg L^{-1}. The thermodynamic parameters of ΔS^0 and ΔH^0 were 148.38 J $mol^{-1}K^{-1}$ and 28.235 kJ mol^{-1}, respectively. The iodine adsorption capacity on C4-750 was 586.30 mg g^{-1}.

ACKNOWLEDGEMENTS

This work is supported by the National High Technology Research and Development Program (863 program 2012 AA 051803) of China and the characterization of the samples by the Analytic and Testing Center of Sichuan University is acknowledged.

REFERENCES

1. L. Wang, Y. Guo, Y. Zhu, Y. Li, Y. Qu, C. Rong, X. Ma and Z. Wang, *Bioresour. Technol.*, **101**, 9807 (2010).
2. C. Michailof, G. Stavropoulos and C. Panayiotou, *Bioresour. Technol.*, **99**, 6400 (2008).
3. M.G. Krivova, D.D. Grinshpan and N. Hedin, *Colloids Surf. A*, **436**, 62 (2013).
4. Q. Jia and A.C. Lua, *J. Anal. Appl. Pyrolysis*, **83**, 175 (2008).
5. V. Subramanian, C. Luo, A.M. Stephan, K.S. Nahm, S. Thomas and B. Wei, *J. Phys. Chem. C*, **111**, 7527 (2007).
6. O. Ioannidou and A. Zabaniotou, *Renew. Sustain. Energy Rev.*, **11**, 1966 (2007).
7. M.A. Lillo-Rodenas, D. Cazorla-Amoros and A. Linares-Solano, *Carbon*, **41**, 267 (2003).
8. Y. Guo, S. Yang, K. Yu, J. Zhao, Z. Wang and H. Xu, *Mater. Chem. Phys.*, **74**, 320 (2002).
9. Q. Lu, X. Yang and X. Zhu, *J. Anal. Appl. Pyrolysis*, **82**, 191 (2008).
10. D. Li, D. Chen and X. Zhu, *Bioresour. Technol.*, **102**, 7001 (2011).
11. H. Liu, G. Li and C. Hu, *J. Mol. Catal. Chem.*, **377**, 143 (2013).
12. Y. Liu, Y. Guo, W. Gao, Z. Wang, Y. Ma and Z. Wang, *J. Clean. Prod.*, **32**, 204 (2012).
13. E. Lorenc-Grabowska, G. Gryglewicz and M.A. Diez, *Fuel*, **114**, 235 (2013).
14. B.K. Pradhan and N.K. Sandle, *Carbon*, **37**, 1323 (1999).
15. I.O. Ali, A.M. Hassan, S.M. Shaaban and K.S. Soliman, *Sep. Purif. Technol.*, **83**, 38 (2011).
16. X. Song, Y. Zhang and C. Chang, *Ind. Eng. Chem. Res.*, **51**, 15075 (2012).
17. S. Brunauer, L.S. Deming, W.E. Deming and E. Teller, *J. Am. Chem. Soc.*, **62**, 1723 (1940).
18. H.H. Tseng, M.Y. Wey and C.H. Fu, *Carbon*, **41**, 139 (2003).

19. L.J. Kennedy, J.J. Vijaya and G. Sekaran, *Ind. Eng. Chem. Res*., **43**, 1832 (2004).
20. C.T. Yu, W.H. Chen, L.C. Men and W.S. Hwang, *Ind. Crops Prod*., **29**, 308 (2009).
21. M. Bystrzejewski and K. Pyrzynska, *Colloids Surf. A*, **377**, 402 (2011).
22. S. Timur, I.C. Kantarli, S. Onenc and J. Yanik, *J. Anal. Appl. Pyrolysis*, **89**, 129 (2010).
23. Q. Qian, Q. Chen, M. Machida, H. Tatsumoto, K. Mochidzuki and A. Sakoda, *Appl. Surf. Sci*., **255**, 6107 (2009).
24. K. Zhu, H. Fu, J. Zhang, X. Lv, J. Tang and X. Xu, *Biomass Bioenergy*, **43**, 18 (2012).
25. N. Tancredi, N. Medero, F. Moller, J. Piriz, C. Plada and T. Cordero, *J. Colloid Interf. Sci*., **279**, 357 (2004).
26. N. Böke, Z.G. Godongwana and L.F. Petrik, *J. Porous Mater*., **20**, 1153 (2013).
27. J. Zhang, H. Fu, X. Lv, J. Tang and X. Xu, *Biomass Bioenergy*, **35**, 464 (2011).
28. G. Moussavi and R. Khosravi, *Chem. Eng. Res. Des*., **89**, 2182 (2011).
29. Y. Li, Z. Di, J. Ding, D. Wu, Z. Luan and Y. Zhu, *Water Res*., **39**, 605 (2005).
30. P. Wang, M. Cao, C. Wang, Y. Ao, J. Hou and J. Qian, *Appl. Surf. Sci*., **290**, 116 (2014).
31. H. Teng and C.T. Hsieh, *Ind. Eng. Chem. Res*., **37**, 3618 (1998).